A novel MAV with treadmill motion of wing

Iman Samani[a)] and Ahmad Sedaghat[b)]
Department of Mechanical Engineering, Isfahan University of Technology, Isfahan 84156-83111, Iran

(Received 10 June 2013; accepted 21 July 2013; published online 10 November 2013)

Abstract The Magnus effect is well known phenomena for producing high lift values from spinning symmetrical geometries such as cylinders, spheres, or disks. But, the Magnus force may also be produced by treadmill motion of aerodynamic bodies. To accomplish this, the skin of aerodynamic bodies may circulate with a constant circumferential speed. Here, a novel wing with treadmill motion of skin is introduced which may generate lift at zero air speeds. The new wing may lead to micro aerial vehicle configurations for vertical take-off or landing. To prove the concept, the NACA0015 aerofoil section with circulating skin is computationally investigated. Two cases of stationary air and moving air are studied. It is observed that lift can be generated in stationary air although drag force is also high. For moving air, the lift and drag forces may be adopted between the incidence angles 20° to 25° where lift can posses high values and drag can remain moderate. © *2013 The Chinese Society of Theoretical and Applied Mechanics.* [doi:10.1063/2.1306202]

Keywords micro aerial vehicle (MAV), Magnus effect, treadmill motion, high angle of attack, aerofoil flows

The first successful device based on Magnus effect was reported in the year of 1924, when Anton Flettner has manufactured the first ship operating with Magnus force using two large cylinders to propel his ship, Buckau. Since that success, the potential of producing high lift forces by rotating bodies in comparison with low lift force values of aerofoil type devices has attracted many researchers in different fields of engineering. Many patents have been registered in the areas of naval or aerospace applications which claimed the use of the Magnus effect and many research results have been published merely based on the generation of aerodynamic forces from the rotating cylinders. But, very few devices were operated successfully.[1]

Recently, the Flettner type rotor is becoming again a hot topic in naval engineering because of the energy costs and the rise of problems with climate change.[1] A comprehensive review of the Magnus effect devices in aeronautics was given by Seifert[1] who believes "today, there are no specific methods available on how to design the lifting device of a rotor airplane or the rotor airplane airframe." Anton Flettner invented the treadmill principle, the usage of a moving surface around an aerofoil, in the year 1923 for ship and airplane applications, which was granted by a German patent.[2] However, to our knowledge, no computational or experimental efforts were made towards analysis and simulation of circulating aerofoils. Instead, many researches were conducted to study spinning cylinders such as using spinning cylinders in the leading or trailing edges of aerofoils as shown in Fig. 1.[3]

Other research were purely conducted to obtain lift and drag of spinning cylinders.[4–10] Seifert[1] has stressed that up to now, there are no specific methods available on how to design the lifting device of a rotor airplane

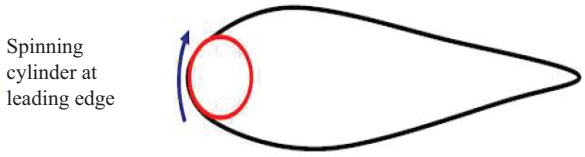

Fig. 1. Rotating cylinder in wing configuration.

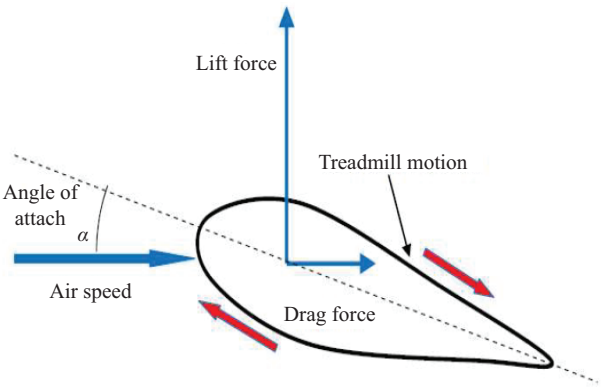

Fig. 2. The schematic of a fixed wing with treadmill motion.

or the rotor airplane airframe and new design methods that can show performance of a rotor airplane during flight are required. Moreover, he insists that the negative Magnus force or gyroscopic effects in the case of especially micro aerial vehicles must be considered because their flights occur at low Reynolds numbers.

In this paper, the possibility of using Magnus force in micro aerial vehicles with a circulating fixed wing is investigated. A schematic of the wing is shown in Fig. 2.

The purposes of this study were two folds. First, we investigated if the circulating wing surfaces generate higher lift than non-circulating surfaces. Second, we investigated if a vertical take-off is possible at zero air speeds. For these purposes, a fluid flow solver was used

a)Email: imansamani2020@yahoo.com.
b)Corresponding author. Email: sedaghat@cc.iut.ac.ir.

to solve The Reynolds average Navier–Stokes (RANS) equations in a C-type mesh around the wing sections. The wing cross section is assumed to be the NACA0015 aerofoil as a test case to be examined for the possibility of the new targets.

Sedaghat and Shahpar[11] have developed a class of high resolution, total variation diminishing (TVD) scheme to solve the governing fluid flow equations around two dimensional aerofoil flows. The RANS equations of the governing compressible flows in conjunction with Baldwin–Lomax turbulence model is solved in general coordinate system using the implicit, time marching, and second order accurate TVD scheme.[11] The method is extension, for solving viscous compressible flows, of the original upwind and symmetric TVD schemes developed by Yee[12] for computation of inviscid flows. An algebraic-hyperbolic grid generator is used to generate C-type orthogonal meshes around aerofoil sections with proper clustering of mesh points in the boundary layer.

In this case, the NACA0015 is merely circulating in a motionless air medium. Based on a non-dimensional speed of treadmill motion of 0.2, 0.5, 1.0, 3.0, and 5.0, the computational results of lift and drag coefficients are shown in Fig. 3 for the aerofoil at different incidence angles of $0°, 5°, 10°, 15°$, and $20°$. The dimensionless treadmill speed is the ratio of circulating speed of the aerofoil to the reference cruise speed of MAV. The angle of attach (AoA) is defined as the angle between the chord line and the horizontal axis (the axis of air speed in none stationary case) as shown in Fig. 2. Here, lift and drag coefficients are defined as

$$C_{\mathrm{L}} = \frac{L}{\frac{1}{2}\rho c U_{\mathrm{cruise}}^2}, \; C_{\mathrm{D}} = \frac{D}{\frac{1}{2}\rho c U_{\mathrm{cruise}}^2}. \tag{1}$$

In Eq. (1), ρ is the air density, c is the aerofoil chord length, and U_{cruise} is a typical cruise speed of MAV. Here, L is the lift force defined in vertical direction as sketched in Fig. 2, which is calculated from the cumulative forces of pressure and shear stress over aerofoil surfaces. For the moving aerofoil, the lift force is in normal direction of air speed. Similarly, drag force D is defined here as cumulative forces of pressure and shear stress in horizontal direction. This is generally defined as the force in direction of air speed for moving aerofoils as shown in Fig. 2.

In order to computationally model stationary air around circulating aerofoil, the free stream velocity is assumed as the cruise speed; however, the aerofoil surface boundary condition is employed such that the aerofoil is also translating with the same cruise speed away from the air speed. From a viewer on the aerofoil surface, zero speed is detected from free stream.

As shown in Fig. 3, the results indicate that by increasing the treadmill speed the lift coefficient has increased; although, the drag coefficients also increases by treadmill speeds at high AoA of 10° and above. For lower incidence angles than 10°, the lift and drag coefficients are decreasing functions of the treadmill speed;

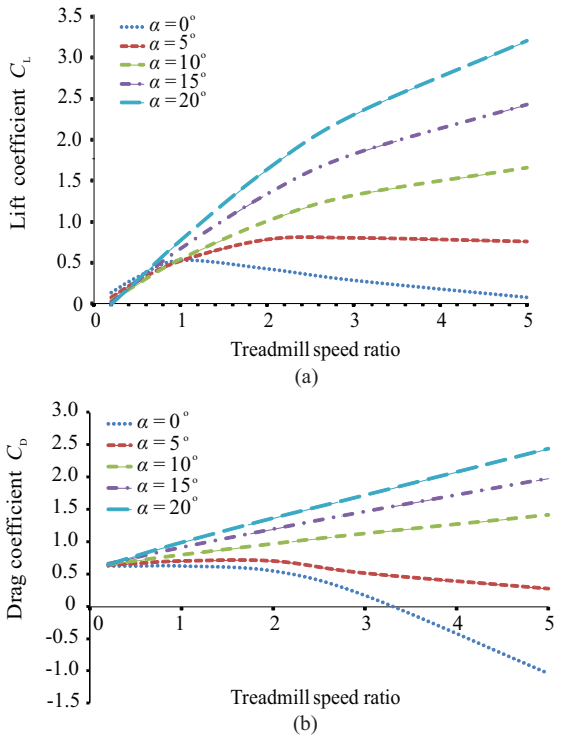

Fig. 3. Lift and drag coefficients with different treadmill speeds in stationary air.

whether this range can be used to produce sufficient lift for a vertical take-off MAV needs to be further investigated using experimental approaches. Hence, the proposed treadmill motion is at least proven that can produce lift at zero air speeds but its magnitude and the corresponding drag should be further studied towards vertical take-off/landing of MAV configurations.

Figure 4 shows an example of streamlines and pressure distribution around the circulating aerofoil at zero incidence angle and dimensionless circulating speed of 3. As seen in this figure, the streamlines (Fig. 4(a)) get closer near trailing edge to speed up the flow which may cause a higher pressure region near the leading edge. This is better seen in Fig. 4(b) for pressure distribution which shows that the lower part of the aerofoil constitutes two zones: one high pressure zone near the leading edge and another low pressure part with a large separation zone appears on the rest lower part till the trailing edge. The pressure distribution looks like the flow situations as air arrives with an incident angle. Thus, the generation of lift by circulating aerofoils in stationary air may be interpreted as pushing air by viscous effects from the upper and lower sides of aerofoil towards the lower part of leading edge where pressure increases and produces the resultant lift and drag forces.

In this case, the NACA0015 aerofoil surface is circulating in a low speed flow. Based on different speed of treadmill motion to air speed (0.2, 0.5, 1.0, 2.0, 3.0, and 5.0), the computational results reveal higher

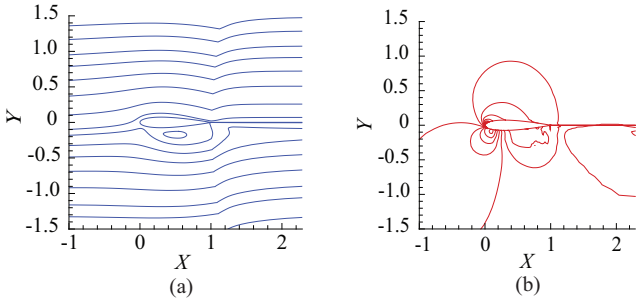

Fig. 4. (a) Streamlines and (b) pressure distributions around the circulating NACA0015 aerofoil at zero incident angle and the dimensionless circulating speed of 3 in stationary air.

lift and drag coefficients at even very high stall incidence angles of up to 35°. Figure 5 shows the results of lift coefficient at different incidence angles of $0°, 5°, 10°, 15°, 20°, 25°, 30°$, and $35°$ by varying the treadmill speed. It is observed that the lift distribution converges to a nearly envelope at the incidence angle of 25°. Generally speaking, higher treadmill speeds lead to higher lift coefficient. Drag coefficient remains marginal up to the incident angle of 15° (below 0.1) and becomes negative at high treadmill speeds; however, for higher AoA the drag force becomes considerable. Figure 6 shows an example of streamlines and pressure distribution around the circulating aerofoil at zero incidence angle and dimensionless circulating speed of 3 in forward flight. As seen in this figure, the streamlines (Fig. 6(a)) are uniformly passes over the aerofoil surface except near lower surface where a separation zone is detected. The high pressure zone is more pronounced as seen in Fig. 6(b) in the lower leading edge which clearly shows a non-uniform distribution of pressure due to circulating effect of aerofoil surfaces. Here, both pressure and viscous effects are acting effectively in both sides of the aerofoil surfaces leading to higher lift force but lower drag force. These findings however, require experimental testing in wind tunnel to confirm validity of the computational results.

The subject of using Magnus force from rotating bodies is fascinating many engineers and scientists to design innovative devices in aerospace and naval engineering. There is a renew interest in Flettner type ships in naval engineering due to increasing trends of fossil fuel costs and climate change concerns. This paper is particularly concerns with a novel fixed wing with treadmill motion to assess possibility of vertical take-off and landing. The computational results for NACA0015 aerofoil reveals that it is possible to obtain lift from the circulating wing in stationary air. Moreover, the results indicate that it is possible to optimise lift to drag ratios by varying incidence angles. Further work is under progress to find an optimum treadmill wing for a vertical take-off/landing MAV and for cruise speeds.

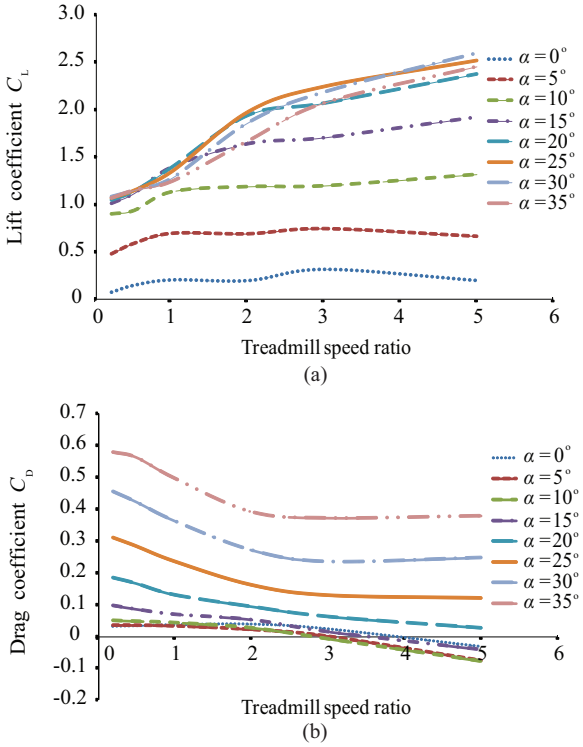

Fig. 5. Lift and drag coefficients with different treadmill speeds in moving air.

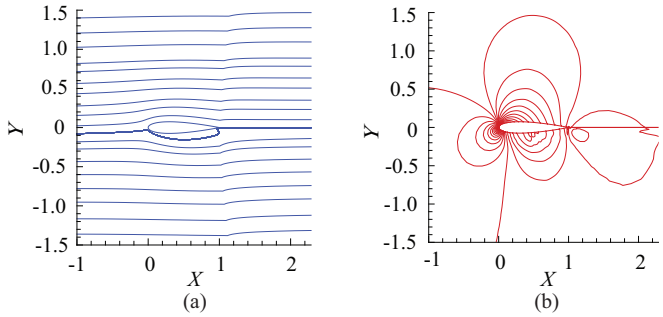

Fig. 6. (a) Streamlines and (b) pressure distributions around the circulating NACA0015 aerofoil at zero incident angle and the dimensionless circulating speed of 3 in moving air.

1. J. Seifert, Progress in Aerospace Sciences **55**, 17 (2012).
2. A. Flettner, German patent, No. 420840 (1923).
3. E. G. Reid, *Tests of rotating cylinders*, Technical Note No. 209, National Advisory Committee for Aeronautics (1925).
4. M. B. Glauert, J. Fluid Mech. **89**, 2 (1957).
5. D. B. Ingham, Computers & Fluids **11**, 351 (1983).
6. S. Mittal and B. Kumar, Journal of Fluid Mechanics **476**, 303 (2003).
7. P. Tokumaru and P. Dimotakis, J. Fluid Mech. **224**, 77 (1991).
8. C. Badalamenti and S. A. Prince, AIAA, 2008-7063 (2008).
9. N. Thouault, C. Breitsamter, J. Seifert, et al., *Numerical analysis of a rotating cylinder with spanwise discs*. Proceeding of the 27th International Congress of the aeronautical Sciences, Nice (2010).
10. L. Labraga, N. Bourabaa, and T. Berkah. Experiments in Fluids **33**, 488 (2002).
11. A. Sedaghat and S. Shahpar, Iranian Journal of Science & Technology **22**, 1 (1998).
12. H. C. Yee, J. Comp. Phys. **57**, 327 (1985).